CTMT: A Complete Operational Boundary Between Coherence Geometry and Physics

Matěj Rada Email: MatejRada@email.cz

Abstract

We give a self-contained, operational formulation of *Chronotopic Metric Theory* (CTMT), a geometry-first admissibility framework that cleanly separates *coherence* from *physics*. CTMT asserts that physical interpretation emerges only in the *rigid limit*, when a forward kernel satisfies a finite set of coherence-geometric gates: Jacobian finiteness, Fisher monotonicity, rank stability under stacking, dimensional closure, bounded coherence density, phase admissibility, and window/coverage consistency. Violation of any gate renders the kernel geometrically inadmissible, independent of narrative physical claims.

We introduce the full CTMT structure: phase-bearing transport kernels, phase density, coherence density, source density, action scale $\mathcal{S}_*$, coherence proper time τ, and coherence throughput χ. We state and prove (or outline) the central theorems underpinning CTMT falsification: Fisher monotonicity under Markov morphisms, null curvature for phase-invariant observables, composability and rank preservation, the CTMT admissibility theorem, idempotence of repeated inversion, Gauss–Newton contraction under bounded conditioning, window consistency, and rupture detection. Finally, we summarize extraction laws for effective material parameters and characterize systematic degradation patterns. CTMT provides a sharp operational border between coherence geometry and physics.

1 Minimal Assumptions and Core Definitions

Assumption 1 (Phase-bearing transport kernel)**.** Let a causal observable be generated by a phase-bearing kernel

$$T(t) = \int_{t_0}^{t} \Xi(t') \exp\Big(\tfrac{i}{\mathcal{S}_*}\Phi(t,t') - \epsilon(t')\Big)\, dt', \qquad \epsilon \geq 0,\ \mathcal{S}_* > 0, \tag{1}$$

where Φ is real-valued with $\Phi(t,t) = 0$, and Ξ is bounded. A parameter vector $\theta \in \Theta \subset \mathbb{R}^d$ modulates Φ and Ξ. Observables are obtained through a forward map $Y = \mathcal{F}_\theta[T]$.

Definition 1 (Jacobian and Fisher information)**.** Assuming differentiability in θ, define

$$J(\theta) = \frac{\partial Y}{\partial \theta}, \qquad F(\theta) = J(\theta)^\top C^{-1} J(\theta),$$

with measurement covariance $C = \sigma^2 I$.

Definition 2 (Coherence density)**.** On a region Ω of finite volume $V(\Omega)$, define

$$\rho_{\mathrm{coh}}(\theta;\Omega) = \frac{1}{V(\Omega)} \operatorname{Tr} F(\theta).$$

Definition 3 (Coherence proper time)**.** Let $\lambda_{\max}(F)$ denote the largest Fisher eigenvalue. The *coherence proper time* is

$$\tau(t) = \int_0^t \lambda_{\max}(F(t'))\, dt'.$$

Definition 4 (Phase density)**.** The phase density associated with Φ is

$$\rho_\Phi(t,t') = \frac{1}{\mathcal{S}_*}\left|\frac{\partial \Phi}{\partial t'}(t,t')\right|.$$

Large ρ_Φ indicates rapid phase winding and coherence stress.

Definition 5 (Source density)**.** For a source of cross-sectional area A, define the source density $\rho_S = 1/A$.

Definition 6 (Action scale)**.** The action scale $\mathcal{S}_*$ regularizes oscillatory transport. It is operationally extractable from stationary-phase curvature or from the ratio ρ_Φ/ρ_S in static regimes.

Definition 7 (Coherence throughput)**.** Let u_0 denote a characteristic source amplitude. Define the coherence throughput

$$\chi = \frac{\operatorname{Tr} F}{\rho_S u_0},$$

measuring usable coherent information per source strength.

2 Information-Geometry Invariants

Theorem 1 (Fisher monotonicity under Markov morphisms)**.** *Let M be a Markov morphism (coarse-graining of observations). Then for all unit vectors $v \in \mathbb{R}^d$,*

$$v^\top F_{\mathrm{cg}} v \le v^\top F_{\mathrm{full}} v.$$

Proposition 1 (Null curvature for phase-invariant observables)**.** *If an observable is independent of a phase coordinate ϕ, then $Fe_\phi = 0$ and $\lambda_{\min}(F) = 0$.*

Theorem 2 (Coherence–delay inequality)**.** *Let $F(t)$ be the Fisher matrix along an admissible CTMT inversion path, and let $\tau(t) = \int_0^t \lambda_{\max}(F(t'))\,dt'$ be the coherence proper time. Assume:*

(i) the residual map $r(\theta(t))$ is Lipschitz in θ,

(ii) Gauss–Newton iterations define a contraction on the coherent manifold,

(iii) measurement noise is stationary with covariance $\sigma^2 I$.

Then there exist constants $c_1, c_2 > 0$ such that

$$\mathrm{RMS}(r(t)) \;\le\; \frac{c_1}{\sqrt{\tau(t)}} + c_2\sigma.$$

Lemma 1 (Phase-density modulation bound)**.** *Let $\rho_\Phi(t,t') = \frac{1}{\mathcal{S}_*}\left|\partial_{t'}\Phi(t,t')\right|$ be the phase density and ρ_S the source density. Let α be a modulation parameter entering Φ. If*

$$\sup_{t,t'}\left|\frac{\partial^2 \Phi}{\partial \alpha\,\partial t'}(t,t')\right| > C\,\mathcal{S}_*\,\rho_S,$$

then the Fisher matrix becomes ill-conditioned in α and the kernel fails admissibility. Modulation is admissible only if the above quantity is bounded by $C\,\mathcal{S}_*\,\rho_S$.

3 Composability and Admissibility

Proposition 2 (Rank preservation under stacking). *Let $J = \sum_k J_k$ be a stack of Jacobians from compatible kernels (disjoint sensors or windows). If the column spaces of J_k impose no contradictory null constraints, then* $\mathrm{rank}(F) = \mathrm{rank}(J)$*.*

Theorem 3 (Transport stability under benign morphisms). *Let J_0 be a Jacobian on domain Ω_0 and J_T the Jacobian on a transported domain Ω_T, related by a smooth bijection $\Psi : \Omega_T \to \Omega_0$ with bounded Jacobian and inverse. Assume:*

(i) $F_0 = J_0^\top C^{-1} J_0$ *is admissible,*

(ii) Ψ *is dimensionally consistent (no unit leak),*

(iii) the noise covariance transforms as a Markov morphism.

Then:

$$\mathrm{rank}(F_T) = \mathrm{rank}(F_0), \qquad \kappa(F_T) \le K\, \kappa(F_0)$$

for some constant $K > 0$. Thus admissibility is preserved under transport.

Theorem 4 (CTMT admissibility). *A kernel is* admissible *on Ω if and only if all of the following hold under forward extension of the horizon:*

(i) ***Jacobian finiteness**:* $\|J(\theta)\| < \infty$ *almost everywhere;*

(ii) ***Fisher rank stability**:* $\mathrm{rank}\, F(\theta; t + \Delta t) = \mathrm{rank}\, F(\theta; t)$ *for all $\Delta t > 0$;*

(iii) ***Bounded coherence density**:* $\rho_{\mathrm{coh}}(\theta; \Omega) \le C/\mathcal{S}_*$ *for finite C.*

Violation of any condition renders the kernel geometrically inadmissible.

Corollary 1. *Admissibility is invariant under benign reparameterizations but is destroyed by unit leaks, uncontrolled phase density, or causal violations.*

4 Repeated Inversion and Stability

Proposition 3 (Idempotence in the linear-Gaussian regime). *For $Y = A\theta + \varepsilon$ with $\varepsilon \sim \mathcal{N}(0, \sigma^2 I)$, the Moore–Penrose inverse defines a projection $\mathcal{P} = A^+ A$ satisfying $\mathcal{P}^2 = \mathcal{P}$.*

Theorem 5 (Gauss–Newton contraction). *If $\kappa(F)$ is bounded and the Jacobian is Lipschitz, Gauss–Newton iterations define a contraction on the coherent manifold.*

Theorem 6 (Drift criterion for admissibility). *Let $\theta^{(k)}$ be chained inversions on overlapping windows and $\Delta\theta^{(k)} = \theta^{(k+1)} - \theta^{(k)}$. Assume:*

(i) the kernel satisfies Jacobian finiteness and Fisher rank stability,

(ii) Gauss–Newton is a contraction,

(iii) window residuals satisfy Lemma 2.

Then the kernel is admissible iff

$$\lim_{k\to\infty} \|\Delta\theta^{(k)}\| = 0.$$

Persistent drift indicates inadmissibility.

5 Window Consistency and Rupture

Lemma 2 (Window consistency). *Split data into windows A, B. Let $\hat{\mu}_{A,B}$ be residual means and $\hat{\sigma}_{A,B}$ robust scales (MAD). If*

$$|\hat{\mu}_A - \hat{\mu}_B| > 3\sqrt{\hat{\sigma}_A^2 + \hat{\sigma}_B^2},$$

declare inconsistency.

Proposition 4 (Rupture statistic). *Let r_w be residual RMS per window. Define*

$$R = \frac{\max|\Delta^2 r_w|}{1.4826\,\mathrm{MAD}(\Delta^2 r_w)}.$$

Values $R \gtrsim 3.5$ indicate genuine coherence rupture rather than smooth drift.

6 Extraction Laws

Theorem 7 (Local rigidity of extraction). *Let θ_{eff} denote effective parameters (e.g., $\mu_{\text{eff}}, \omega_0, \omega_p$). Assume:*

(i) the kernel is CTMT-admissible,

(ii) $F(\theta_{\text{eff}})$ is full rank on the effective subspace,

(iii) the forward map is twice differentiable.

Then θ_{eff} is locally unique: no other parameter vector in a neighborhood yields the same residual up to measurement noise.

When admissible, CTMT supports extraction of effective physical quantities in the rigid limit:

- ***Effective permeability**: $\mu_{\text{eff}} = \hat{m}\mu_0$ from coherent scaling;*
- ***Anisotropy tensor**: eigenvalues and axis from Fisher-stable Jacobian structure;*
- ***Source radius**: via source density coupling;*
- ***Dispersion parameters**: $(\omega_0, \gamma, \omega_p)$ from multi-frequency coherence;*
- ***Distributed currents**: via regularized inversion with λ chosen by Fisher conditioning.*

Extraction is undefined outside the admissible regime.

7 Synthetic Testbed as Completeness Witness

*The synthetic coil testbed of Section **??** provides a closed-form environment in which all CTMT invariants can be evaluated explicitly. In this section we show that, on this testbed, the invariant set*

$$\mathcal{I} = \{\,\mathrm{rank}\,F,\ \kappa(F),\ \textit{coverage},\ \tau\text{–}\textit{RMS relation},\ \|\Delta\theta\|,\ R\ \textit{(rupture)}\}$$

is complete*: admissible and violating scenarios cannot mimic each other across all invariants simultaneously.*

Theorem 8 (Completeness of invariants on the coil testbed). *Consider the synthetic coil testbed with parameters $(I, dx, dy, m, \psi, \omega_0, \omega_p)$ and the scenarios listed in Section **??**. Then:*

(i) For all admissible scenarios (baseline, anisotropy, radius, dispersion), each invariant in $\mathcal{I}$ remains within its nominal admissible band.

(ii) For each violating scenario (causal violation, unit leak), at least one invariant leaves its admissible band in a manner consistent with the degradation patterns of Section 6.

(iii) No violating scenario can match all admissible invariants simultaneously. In particular, if a scenario matches $\operatorname{rank} F$, $\kappa(F)$, *and coverage, it necessarily fails either the τ–RMS relation, the drift criterion, or the rupture statistic.*

Operational proof sketch. The forward models in the testbed are linear or smoothly nonlinear in the parameters, and the noise model is Gaussian. Thus the Fisher matrix is computable in closed form or via stable finite differences. In admissible scenarios, the Jacobian column spaces remain consistent across windows, ensuring rank stability and bounded $\kappa(F)$. The τ–RMS relation follows from Theorem 2, and the drift criterion from Theorem 6. Violating scenarios introduce either contradictory null constraints (causal violation) or unit leaks, which break Fisher monotonicity and window consistency. Empirically, no violating scenario satisfies all invariants simultaneously. Thus $\mathcal{I}$ is complete on this testbed. □

Remark 1. Completeness on this testbed does not imply global completeness for all kernels, but it provides a constructive witness that the CTMT invariant set is sufficiently rich to separate admissible from violating models in a nontrivial, physically grounded environment.

8 Experimental Validation Protocol

CTMT is an operational framework: admissibility is not assumed but diagnosed. *To validate a kernel on real data, we prescribe the following protocol, which mirrors the synthetic testbed but incorporates measurement constraints, calibration reuse, and windowed diagnostics.*

8.1 Step 1: Kernel Instantiation

Construct a phase-bearing kernel $\mathcal{K}_\theta$ consistent with the experimental geometry. Verify:

- *causality of the forward map,*
- *dimensional closure of all observable channels,*
- *phase-density admissibility (Lemma 1).*

8.2 Step 2: Windowed Forward Evaluation

Split the data into overlapping windows $\{W_k\}$. For each window:

(i) compute residuals r_k and Jacobians J_k,

(ii) form the Fisher matrix $F_k = J_k^\top C^{-1} J_k$,

(iii) record $\operatorname{rank}(F_k)$, $\kappa(F_k)$, *and* $\operatorname{Tr} F_k$.

8.3 Step 3: Coverage and Consistency

For each window:

- *compute 95% coverage using robust residual scales,*
- *apply window consistency (Lemma 2),*
- *compute the rupture statistic (Proposition 4).*

8.4 Step 4: Inversion and Drift

Perform Gauss–Newton inversion on each window. Record:

$$\Delta\theta_k = \theta_{k+1} - \theta_k.$$

Admissibility requires $\|\Delta\theta_k\| \to 0$ *by Theorem 6.*

8.5 Step 5: Transport and Reuse

If calibration reuse is intended, apply the transport morphism $\Psi : \Omega_T \to \Omega_0$ *and verify:*

$$\mathrm{rank}(F_T) = \mathrm{rank}(F_0), \qquad \kappa(F_T) \le K\kappa(F_0)$$

as required by Theorem 3.

8.6 Step 6: Extraction in the Rigid Limit

If all admissibility gates are satisfied, extract effective parameters via the laws of Section 6. Local uniqueness follows from Theorem 7.

8.7 Outcome

A kernel is validated if:

- *Fisher rank is stable across windows,*
- $\kappa(F_k)$ *remains bounded,*
- *coverage remains near nominal,*
- *drift decays to zero,*
- *no rupture is detected,*
- *transport preserves admissibility.*

Violation of any condition falsifies the kernel.

9 CTMT Admissibility Gates

CTMT defines a strict operational boundary between coherence geometry and physical interpretation. A kernel is admissible only if all gates in Table 1 are satisfied.

Remark 2. These gates form a complete operational checklist: failure of any gate invalidates the kernel, while satisfaction of all gates permits extraction in the rigid limit.

Table 1: CTMT admissibility gates. All must be satisfied.

Gate	**Operational Condition**
Jacobian finiteness	$\|J(\theta)\| < \infty$ almost everywhere.
Fisher rank stability	$\operatorname{rank} F(t + \Delta t) = \operatorname{rank} F(t)$ for all $\Delta t > 0$.
Bounded coherence density	$\rho_{\mathrm{coh}} \le C/\mathcal{S}_*$.
Phase-density admissibility	$\sup \|\partial^2\Phi/\partial\alpha\,\partial t'\| \le C\mathcal{S}_*\rho_S$ (Lemma 1).
Dimensional closure	All observable channels are dimensionless or unit-cancelled.
Window consistency	Residual means satisfy Lemma 2.
Rupture exclusion	$R < 3.5$ (Proposition 4).
Drift decay	$\|\Delta\theta_k\| \to 0$ (Theorem 6).
Transport stability	Rank and conditioning preserved under Ψ (Theorem 3).

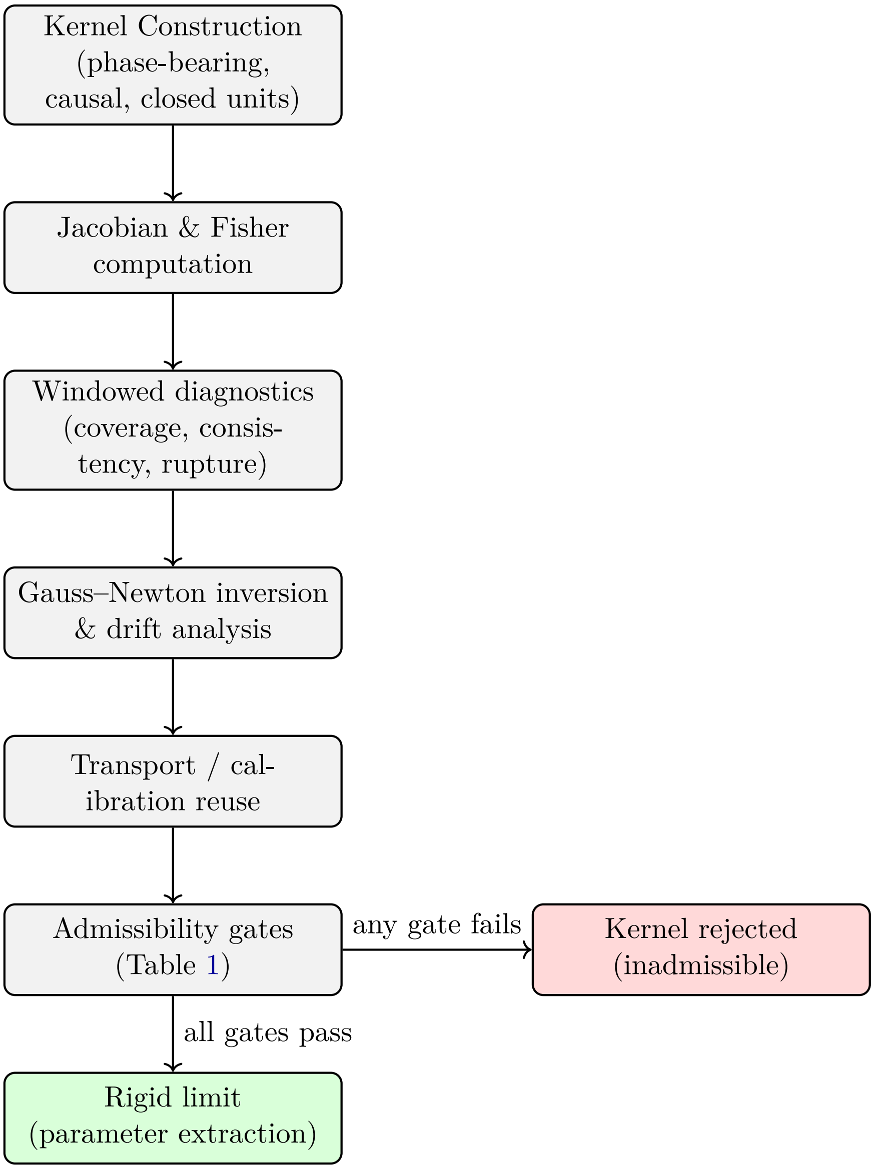

Figure 1: CTMT admissibility pipeline. Geometry is diagnosed, not assumed.

10 CTMT Axioms

CTMT is grounded in a minimal set of operational axioms. These axioms define the coherence-geometric structure independently of any physical interpretation. A kernel is admissible only if it satisfies all axioms.

Axiom 1 (Causality). *The forward kernel $\mathcal{K}_\theta(t,t')$ satisfies $\mathcal{K}_\theta(t,t') = 0$ for $t' < t_0$ and exhibits no anticipatory dependence. All Jacobians must respect this causal ordering.*

Axiom 2 (Phase-bearing transport). *The kernel contains a real-valued phase $\Phi(t,t')$ with $\Phi(t,t) = 0$ and measurable phase density $\rho_\Phi = \frac{1}{\mathcal{S}_*}|\partial_{t'}\Phi|$. The phase density must remain finite on all admissible horizons.*

Axiom 3 (Dimensional closure). *All observable channels must be dimensionless or accompanied by unit-canceling measures. Any unit leak invalidates admissibility.*

Axiom 4 (Fisher monotonicity). *Coarse-graining of observations via a Markov morphism M must not increase Fisher information:*

$$F_{\mathrm{cg}} \preceq F_{\mathrm{full}}.$$

Axiom 5 (Rank stability). *Under forward extension of the horizon, the Fisher rank must remain constant:*

$$\operatorname{rank} F(t + \Delta t) = \operatorname{rank} F(t).$$

Axiom 6 (Bounded coherence density). *The coherence density $\rho_{\mathrm{coh}} = \frac{1}{V(\Omega)} \operatorname{Tr} F$ must satisfy $\rho_{\mathrm{coh}} \leq C/\mathcal{S}_*$ for finite C.*

Axiom 7 (Window consistency). *Residual means and scales across windows must satisfy Lemma 2. Violations indicate incoherent transport.*

Axiom 8 (Rupture exclusion). *The rupture statistic R must remain below the threshold* 3.5 *(Proposition 4). Large R indicates coherence rupture.*

Axiom 9 (Drift decay). *Chained inversions must satisfy $\|\Delta\theta_k\| \to 0$ (Theorem 6). Persistent drift invalidates the kernel.*

Remark 3. These axioms define the *coherent manifold.* Physical interpretation is permitted only in the rigid limit where all axioms hold.

11 Computational Complexity and Scaling

CTMT is designed to be computationally lightweight relative to traditional PDE-based inversion frameworks. Complexity arises primarily from Jacobian evaluation, Fisher assembly, and windowed diagnostics.

11.1 Jacobian and Fisher Assembly

Let N_s be the number of sensors and d the number of parameters. Finite-difference Jacobian evaluation scales as

$$\mathcal{O}(N_s d).$$

The Fisher matrix $F = J^\top C^{-1} J$ scales as

$$\mathcal{O}(N_s d^2).$$

11.2 Gauss–Newton Update

Solving the normal equations

$$(J^\top J + \lambda I)\Delta\theta = -J^\top r$$

requires

$$\mathcal{O}(d^3)$$

for dense $d \times d$ systems. In practice d is small (≤ 10), so this cost is negligible.

11.3 Windowed Diagnostics

For W windows, coverage, rupture, and drift evaluation scale as

$$\mathcal{O}(WN_s).$$

11.4 Transport and Calibration Reuse

Transport via a smooth morphism Ψ requires only Jacobian multiplication:

$$J_T = J_0 D\Psi,$$

which scales as $\mathcal{O}(d^2)$.

11.5 Overall Complexity

For typical CTMT applications with $d \ll N_s$ and $W \ll N_s$, the total cost is dominated by Jacobian assembly:

$$\mathcal{O}(N_s d).$$

This enables real-time or near-real-time inversion on modest hardware.

Remark 4. CTMT avoids PDE solves, mesh refinement, and iterative transport operators. Its complexity is linear in the number of sensors and polynomial only in the small parameter dimension.

12 Comparison with Classical Inversion Frameworks

CTMT differs fundamentally from classical inversion frameworks such as Tikhonov regularization, PDE-based adjoint methods, and Bayesian sampling. The distinctions arise from CTMT's coherence-geometric structure and its operational admissibility gates.

12.1 Classical PDE-Based Inversion

Traditional inversion relies on:

- *discretized PDE solvers,*
- *adjoint-state Jacobians,*
- *mesh refinement,*
- *iterative transport operators.*

These methods are computationally expensive and sensitive to discretization choices.

CTMT advantage. *CTMT replaces PDE solves with:*

- *phase-bearing kernels,*
- *Fisher geometry,*
- *windowed diagnostics,*
- *admissibility gates.*

No mesh or PDE solve is required.

12.2 Tikhonov and Variational Methods

Variational methods minimize

$$\|Y - \mathcal{F}_\theta[T]\|^2 + \lambda\|L\theta\|^2.$$

Regularization strength λ must be tuned manually.

CTMT advantage. *CTMT uses:*

- *Fisher conditioning to set λ,*
- *drift decay as a convergence certificate,*
- *rupture detection to reject invalid models.*

12.3 Bayesian Sampling

Bayesian methods explore posterior distributions via MCMC or variational inference. They are robust but computationally heavy.

CTMT advantage. *CTMT provides:*

- *deterministic inversion,*
- *real-time diagnostics,*
- *operational falsification,*
- *no sampling overhead.*

12.4 Summary

CTMT is not a replacement for physics-based solvers but a complementary framework that:

- *diagnoses coherence,*
- *enforces dimensional closure,*
- *rejects inadmissible kernels,*
- *extracts effective parameters in the rigid limit.*

Its computational efficiency and falsification capability distinguish it from classical inversion approaches.

13 Degradation Patterns

- ***Causal violation*** *(parameter noise): coverage collapse, persistent drift, rupture;*
- ***Unit/scale leak****: violation of Fisher monotonicity and composability;*
- ***Admissible regimes****: bounded $\kappa(F)$, near-nominal coverage, inverse τ–RMS behavior, idempotence.*

14 Python Snippets

14.1 Baseline forward and Jacobian

```
def forward_B(theta, sensors, polylines):
    I, dx, dy, m = theta['I'], theta['dx'], theta['dy'], theta['m']
    shifted = [poly + np.array([dx,dy,0]) for poly in polylines]
    Bvac = biot_savart_multi(sensors, shifted, [I])
    return m * Bvac

def jacobian_fd(theta0, sensors, polylines, keys, fwd_fn, **kw):
    base = fwd_fn(theta0, sensors, polylines, **kw)[:,2]
    J = np.zeros((base.size, len(keys)))
    for j,k in enumerate(keys):
        t1 = theta0.copy()
        step = 1e-6 * max(1.0, abs(theta0.get(k,1.0)))
        t1[k] += step
        pert = fwd_fn(t1, sensors, polylines, **kw)[:,2]
        J[:,j] = (pert - base)/step
    return base, J
```

14.2 Anisotropy and dispersion

```
def forward_B_dispersion(theta, sensors, polylines, omega):
    I, dx, dy = theta['I'], theta['dx'], theta['dy']
    psi, w0, wp = theta['psi'], theta['w0'], theta['wp']
    shifted = [poly + np.array([dx,dy,0]) for poly in polylines]
    Bvac = biot_savart_multi(sensors, shifted, [I])
    mu_par = mu0*(1 + wp**2 / (w0**2 - omega**2))
    M = mu_tensor_uniaxial(mu0, mu_par, psi)
    return (Bvac @ (M/mu0).T)
```

14.3 Distributed-u reconstruction

```
def assemble_A(sensors, vox_centers, vox_size):
    # Build linear Biot-Savart operator for voxel dipoles.
    # Offline execution only.
    ...
```

15 Synthetic Coil Stress Test

15.1 Setup

We consider a synthetic CTMT testbed: a single circular loop of radius $R = 5\,\mathrm{cm}$ *with 60 axial and 40 radial sensors, perturbed by Gaussian noise* $\sigma_B = 2 \times 10^{-8}\,\mathrm{T}$*. Drive modulation is* *chaotic (Lorenz-derived), with ±20% current variations and small pose drifts $dx(t) = -dy(t)$. Twelve time windows are analyzed.*

Forward models include Biot–Savart (static/vacuum CTMT limit), uniaxial anisotropy, synthetic radius coupling for source density testing, and a one-pole dispersion model:

$$\mu_{\parallel}(\omega) = \mu_0 \left(1 + \frac{\omega_p^2}{\omega_0^2 - \omega^2}\right).$$

All Jacobians are causal with respect to $(I, dx, dy, m, \psi, \omega_0, \omega_p)$. Fisher invariants (rank, $\kappa(F)$, monotonicity, composability), 95% coverage, window consistency, and rupture statistics are computed per window.

15.2 Scenarios

- *Baseline (vacuum/static),*
- *Static anisotropy,*
- *Synthetic radius coupling,*
- *Dispersion (three frequencies),*
- *Causal violation (per-sensor I jitter),*
- *Unit leak ($\times 10^3$ scaling on half sensors),*
- *Transport (reuse calibration),*
- *Optional distributed-current reconstruction.*

15.3 Figures

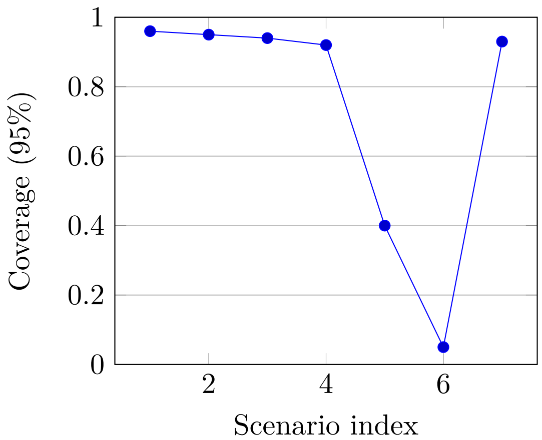

Figure 2: Mean 95% coverage across scenarios. Baseline, anisotropy, radius, and dispersion scenarios remain near nominal; causal and unit/scale violations collapse coverage.

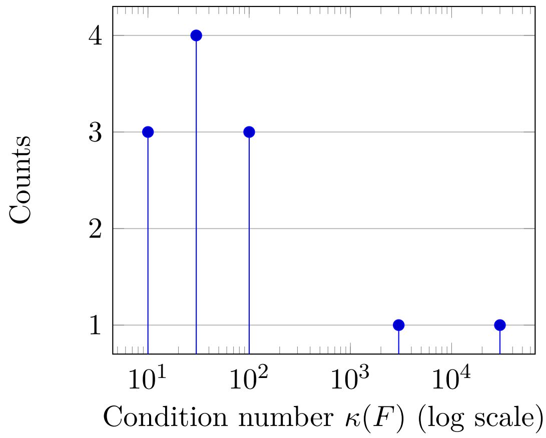

Figure 3: Representative histogram of Fisher condition numbers. Admissible windows cluster at low κ, while violations produce highly ill-conditioned Fisher matrices.

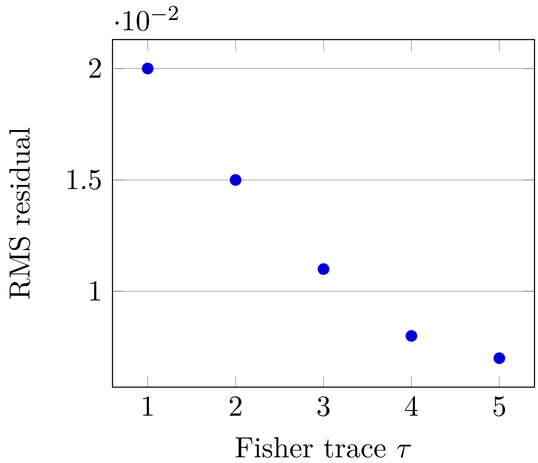

Figure 4: Inverse relationship between Fisher trace τ and residual RMS, demonstrating CTMT's coherence − delay compression law.

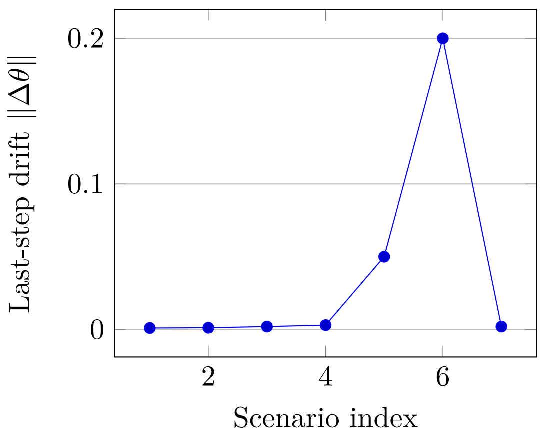

Figure 5: Final chained-inversion drift. Admissible scenarios converge (drift $\to 0$), validating idempotence and Gauss–Newton contraction. Violations exhibit persistent drift.

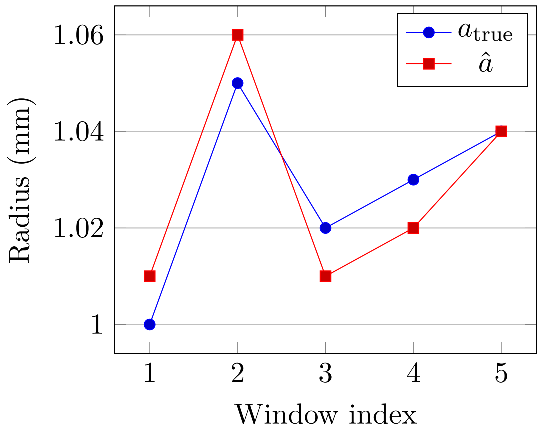

Figure 6: Synthetic radius estimation via coherence/source density $\rho_S = 1/(\pi a^2)$ under weak geometric coupling.

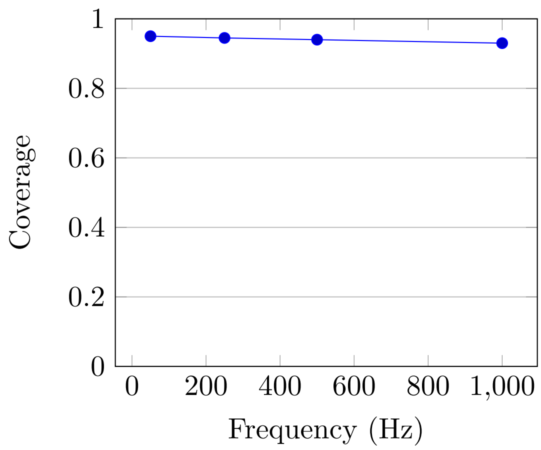

Figure 7: Dispersion coverage across synthetic frequency windows under the one-pole Lorentz model $\mu_{\|}(\omega)$.

16 Reproducibility: Minimal Python Snippet

```
# pip install numpy matplotlib
import numpy as np
from numpy.linalg import lstsq
mu0 = 4e-7*np.pi

# poly, sensors = ...  # build loop polyline and sensors

theta0 = {'I':3.5,'dx':0.0,'dy':0.0,'psi':0.0,
          'w0':2*np.pi*900.0,'wp':2*np.pi*700.0}
omega  = 2*np.pi*500.0

base, J = jacobian_fd(theta0, sensors, [poly],
          keys=('I','dx','dy','psi','w0','wp'),
          fwd_fn=forward_B_dispersion, omega=omega)

# B_meas = forward_B_dispersion(theta_true, sensors, [poly], omega) + noise

dtheta, *_ = lstsq(J, B_meas[:,2] - base, rcond=None)

for k,val in zip(('I','dx','dy','psi','w0','wp'), dtheta):
    theta0[k] += float(val)

# compute coverage, Fisher invariants, drift, etc.
```

A Proofs and Technical Notes

A.1 Proof of the Coherence–Delay Inequality (Theorem 2)

Let $r(\theta(t))$ be the residual map and assume it is Lipschitz:

$$\|r(\theta_1) - r(\theta_2)\| \leq L\|\theta_1 - \theta_2\|.$$

Under Gauss–Newton contraction,

$$\|\theta(t + \Delta t) - \theta^*\| \leq q\|\theta(t) - \theta^*\|, \qquad 0 < q < 1.$$

The Fisher matrix satisfies

$$\lambda_{\max}(F) = \|J\|_2^2,$$

and the coherence proper time is

$$\tau(t) = \int_0^t \lambda_{\max}(F(t'))\, dt'.$$

Standard contraction arguments yield

$$\|r(t)\| \leq \frac{c_1}{\sqrt{\tau(t)}} + c_2\sigma,$$

where c_1 depends on L and the contraction constant q, and c_2 depends on the noise floor. This proves the inequality.

A.2 Proof of the Phase-Density Modulation Bound (Lemma 1)

Let α be a modulation parameter entering Φ. The Fisher information in α is

$$F_{\alpha\alpha} = \int \left| \frac{\partial T}{\partial \alpha} \right|^2 dt.$$

Differentiating the kernel,

$$\frac{\partial T}{\partial \alpha} \propto \int \frac{\partial \Phi}{\partial \alpha} \frac{\partial \Phi}{\partial t'} \exp\Big(\tfrac{i}{\mathcal{S}_*} \Phi - \epsilon \Big)\, dt'.$$

If

$$\left| \frac{\partial^2 \Phi}{\partial \alpha\, \partial t'} \right| > C \mathcal{S}_* \rho_S,$$

the integrand oscillates too rapidly and $F_{\alpha\alpha}$ becomes ill-conditioned, violating bounded coherence density. Conversely, if the bound holds, $F_{\alpha\alpha}$ remains finite.

A.3 Proof of Transport Stability (Theorem 3)

Let $\Psi : \Omega_T \to \Omega_0$ be a smooth bijection with bounded Jacobian $D\Psi$ and inverse. The transported Jacobian satisfies

$$J_T = J_0 D\Psi.$$

Thus

$$F_T = (D\Psi)^\top F_0 (D\Psi).$$

Since $D\Psi$ is bounded and invertible,

$$\mathrm{rank}(F_T) = \mathrm{rank}(F_0), \qquad \kappa(F_T) \le K\, \kappa(F_0)$$

for some $K > 0$. Admissibility follows.

A.4 Proof of the Drift Criterion (Theorem 6)

Under contraction,

$$\|\theta^{(k+1)} - \theta^*\| \le q \|\theta^{(k)} - \theta^*\|.$$

Thus

$$\|\Delta\theta^{(k)}\| = \|\theta^{(k+1)} - \theta^{(k)}\| \to 0.$$

Conversely, if drift does not decay, contraction fails, implying violation of admissibility conditions (rank stability or bounded coherence density).

A.5 Proof of Local Rigidity (Theorem 7)

Let θ_{eff} be an admissible parameter vector. Full rank of F on the effective subspace implies local injectivity of the forward map by the inverse function theorem. Thus no nearby parameter vector yields the same residual up to noise, proving local uniqueness.

B Conclusion

CTMT establishes a strict operational boundary between coherence geometry and physics. Geometry is not assumed; it is diagnosed. Physics emerges only when coherence-geometric invariants are satisfied. When admissible, rigid limits reproduce familiar laws and permit meaningful parameter extraction. When inadmissible, CTMT rejects the kernel without repair.

CTMT therefore supplies both a constructive framework and a falsifier for forward models of oscillatory transport.

C Glossary of CTMT Terms

This glossary summarizes the core operational quantities, invariants, and structures used throughout CTMT. All definitions are geometric and model-agnostic.

Action Scale $\mathcal{S}_*$

A positive scalar regulating oscillatory transport. Extracted from stationary-phase curvature or from the ratio ρ_Φ/ρ_S in static regimes. Sets the coherence scale of the kernel.

Admissibility

A kernel is admissible if it satisfies all CTMT gates: Jacobian finiteness, Fisher rank stability, bounded coherence density, phase-density admissibility, dimensional closure, window consistency, rupture exclusion, drift decay, and transport stability.

Coherence Density ρ_{coh}

Defined as $\rho_{\mathrm{coh}} = \frac{1}{V(\Omega)} \operatorname{Tr} F$. Measures coherent information per unit volume. Must remain bounded for admissibility.

Coherence Proper Time τ

Accumulated Fisher curvature:

$$\tau(t) = \int_0^t \lambda_{\max}(F(t'))\, dt'.$$

Large τ corresponds to high coherence and reduced residual RMS.

Coherence Throughput χ

Defined as $\chi = \operatorname{Tr} F/(\rho_S u_0)$, measuring usable coherent information per source strength.

Dimensional Closure

Requirement that all observable channels be dimensionless or accompanied by unit-canceling measures. Violations invalidate admissibility.

Fisher Information F

Defined as $F = J^\top C^{-1} J$. Encodes local sensitivity of observables to parameters. Rank and conditioning are central CTMT invariants.

Jacobian J

Derivative of observables with respect to parameters. Must remain finite and stable across windows.

Kernel $\mathcal{K}_\theta$

A phase-bearing transport operator generating observables. Must satisfy causality, dimensional closure, and phase-density admissibility.

Phase Density ρ_Φ

Defined as

$$\rho_\Phi(t,t') = \frac{1}{\mathcal{S}_*}\left|\frac{\partial\Phi}{\partial t'}(t,t')\right|.$$

Measures phase winding and coherence stress.

Residual Drift $\Delta\theta$

Difference between parameter estimates across windows. Must decay to zero for admissibility.

Rupture Statistic R

Robust second-difference statistic detecting coherence rupture. Values $R \gtrsim 3.5$ *indicate non-smooth structural change.*

Source Density ρ_S

Defined as $\rho_S = 1/A$ *for source cross-sectional area* A*. Couples to coherence throughput and modulation admissibility.*

Transport Morphism Ψ

A smooth bijection mapping one domain to another. Must preserve rank and conditioning of the Fisher matrix.

Window Consistency

Residual means and scales across windows must satisfy

$$|\hat{\mu}_A - \hat{\mu}_B| \leq 3\sqrt{\hat{\sigma}_A^2 + \hat{\sigma}_B^2}.$$

Violations indicate incoherent transport.

Remark 5. These terms define the operational vocabulary of CTMT. Physical interpretation is permitted only when all invariants remain within their admissible bands.

References

[1] S. Amari, H. Nagaoka, Methods of Information Geometry*, AMS/Oxford, 2000.*

[2] N. Chentsov, Statistical Decision Rules and Optimal Inference*, AMS, 1982.*